Proceedings Paper:

Zhang, T., Ballantyne, E.E.F. orcid.org/0000-0003-4665-0941 and Stone, D.A. orcid.org/0000-0002-5770-3917 (2019) Fully integrated EV energy storage using transport infrastructure. In: 2019 International Conference on Clean Electrical Power (ICCEP). 2019 International Conference on Clean Electrical Power (ICCEP), 02-04 Jul 2019, Otranto, Italy. Institute of Electrical and Electronics Engineers (IEEE) , pp. 337-344. ISBN 9781728113579

https://doi.org/10.1109/iccep.2019.8890133

Fully integrated EV energy storage using transport infrastructure

T. Zhang *, E. E. F. Ballantyne **, and D. A. Stone *

*Department of Electronic and Electrical Engineering, The University of Sheffield, 3 Solly Street, Sheffield, S1 4DE, UK

** Management School, The University of Sheffield, Conduit Road, Sheffield, S10 1FL, UK

Abstract— **This paper explores the synergy between the use of electric vehicles (EVs) for commuting and light rail systems, for example an inner city trams system. The desire to move towards EVs is rapidly increasing the number of EVs available on the roads, and hence the availability of EV batteries for future vehicle to grid (V2G) applications. Most Light rail systems utilize a DC power supply (typically 750Vdc) and require large power draw as the tram / train accelerates. Moreover, a large regenerative power results when the tram / train stops. This paper explores the typical energy use in light rail systems and explores the utilization of the dc rail supply to charge EV's parked in 'park-and-ride' facilities trackside. In addition, the V2G aspect of the system could allow the EV battery to form an energy supply to assist the tram / train during acceleration and accept the regenerated energy from the system as the tram / train stops.**

Index Terms—**tram, regenerative braking energy, energy storage system, vehicle-to-grid.**

I. Introduction

The UK set the target for 2050, to cut carbon emissions to at least 80% below the 1990 level [1]. By 2017, the total GHG and CO_2 emission of UK has been reduced to 43% and 38% below the 1990 level, respectively [2]. Following efforts to reduce GHG emissions in the energy sector, transport is now the largest contributor of emissions in the UK. In 2017, 34% of the total CO_2 emissions in the UK came from transport, with road transport being the most significant source [2].

Electrification of the transport sector, especially urban light-rail networks is now considered an essential measure towards GHG reduction target and tackling increasing environmental pollution [3]. Although the urban rail system is more energy efficient than cars, the energy consumption is still substantial [4]. Because the operational period of the passenger rail service may overlap with the peak generation period (from approximately 07:00 to 20:00) of the grid [5], the electrification of the rail network may stress the grid to some extent in these periods. Therefore, how to reduce the light-rail electricity consumption during the peak generation and ease the stress of the grid, is a problem to be addressed.

Besides, improving the energy efficiency of the light-rail system is also an important measure towards the GHG reduction goal. When a tram decelerates, energy is produced and returned to the network. This is commonly called regenerative energy. If there is another tram in the same track section, the second tram can utilize the regenerated energy, lowering the energy drawn from substations and the utility supply. However, if there are no other trams in the section, the regenerated energy is often dumped into resistor banks, either on-board the tram or lineside, as the substations are generally simple unidirectional rectifiers. This regenerated energy causes the voltage at the tram to rise uncontrollably and could potentially damage the network / tram if resistive dumping of the regenerated energy is not carried out. If this energy was recovered and utilized, the energy efficiency of a light-rail system would be improved.

Additionally, given the growing number of available electric vehicles (EVs) [6], and the precept that EVs will be left in park-and-ride facilities while owners commute into the city center [7-9], there is a growing opportunity to utilize static EVs as the line side storage for the tram network. EVs could then store the braking, or regenerative, energy when the tram /train is braking and provide that energy back when the tram /train is accelerating, and even provide their unused electrical energy to the rail network during peak grid demand periods. Thus, this paper mainly studies the methodology for connecting road and rail for overall energy integration. The Supertram network in Sheffield (UK) is chosen as the research subject for the study, and a model of it is constructed in MATLAB-Simulink. The energy balance of the network, including the energy supplied from the substations, the regenerated energy dissipated on the dump resistors, and the regenerated energy utilized by other trams is investigated over the whole network. The model is then expanded to investigate the addition of EV batteries, which serve as stationary energy storage located in the park and ride facilities to the tram network. The improvement of the energy balance is then explored for the network.

II. Tram Operation System

The Supertram is a light rail network operated by Stagecoach company. It provides inner-city rail public transportation service to Sheffield city (UK). As a focus of this study, it is considered as a typical urban light rail tram network.

This work was supported by the Grantham Centre for Sustainable Futures, University of Sheffield, Sheffield, S10 2TN, UK.

The total route length of the tram system is 29 km. It consists of three routes, the blue line, the yellow line and the purple line as shown in Fig.1. In the network, each track is a dual rail system allowing inward and outward travel from the city center, and where routes overlap, the dual track is shared between routes, through timetabling of the services. There are in total 48 stops in the network. The official park-and-ride facilities are located at Halfway, Meadowhall, Valley Centertainment, Nunnery Square and Middlewood tram stops.

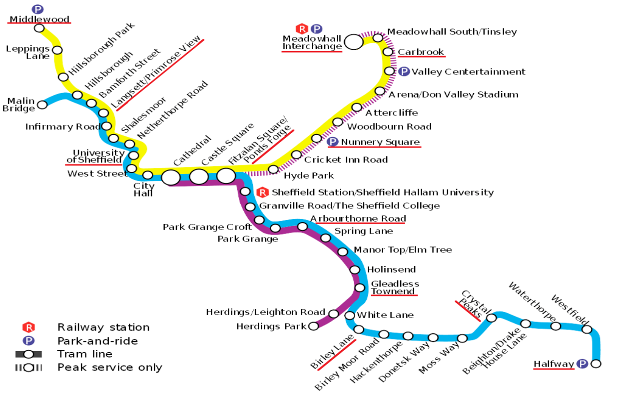

Fig. 1. Sheffield Supertram system (Red underlined stops are electricity substations)

The system operates on a nominal 750V dc supply. The 750Vdc being supplied via a transformer and rectifier arrangement from the 11kV utility grid at the various network substations, shown with their names underlined in red in Fig. 1.

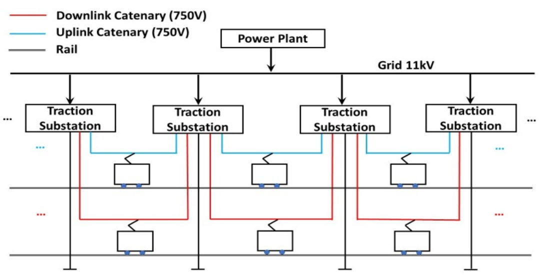

Fig. 2. Tram power supply configuration

The substation is operated with a bilateral power supply. Namely, each substation supplies power to the two adjacent sections. There are downlink tracks and uplink tracks in each section. Fig.2 shows the full system layout.

According to the timetable of the Supertram, the departure interval of each route is larger than 10 minutes. The time used for travelling through two adjacent substations is typically less than 10 minutes. Therefore, if there is only one route passing through two adjacent substations, there is always only one tram traveling on either the uplink or downlink at any given time, and hence all the regenerative electricity will be wasted. If there is more than one route passing through two adjacent substations, it is possible that two trams will be travelling in the same direction at a time, and hence the regenerative energy can possibly be reused.

As shown in Fig. 1, only the section between Langsett and Gleadless Townend will have more than two tramcars travelling in the same direction between two adjacent substations at any given time. The other sections only have one tramcar travelling on either the uplink or the downlink at a time.

III. Input Data

In this study, a simple energy model based on the collected operational data of the tramcar is used to calculate instantaneous energy use, and from that, overall system energy balance.

A. Operational data of tramcar

The tram system in Sheffield runs along the road for sections of the track, and therefore traffic conditions influence the power consumption of individual journeys. The energy usage of the trams in this study was calculated based on real-world GPS data logging of position, velocity and acceleration of the trams. Six sets of GPS data were collected on both morning and afternoon on three different days. This allowed an average consumption to be estimated, alongside actual journey data. Since there is limited space in this paper, only a set of velocity and distance data of a journey from Halfway to Malin Bridge is shown in Fig. 3 for demonstration.

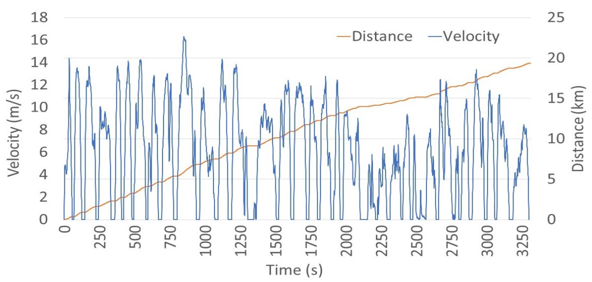

Fig. 3. The change of velocity and distance over time during the journey from Halfway to Malin Bridge

It is worth noting that the change of height above mean sea level has an influence on the power consumption. Data of the height above mean sea level was also collected. A set of the height above mean sea level and distance data of a journey from Halfway to Malin Bridge is shown in Fig. 4 for demonstration. The tram stop locations are highlighted with red dots.

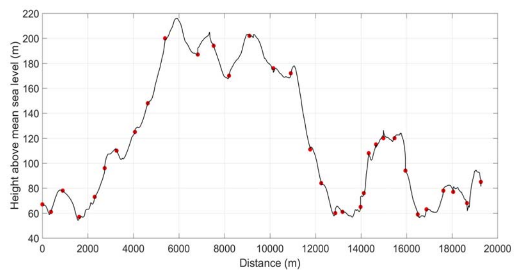

Fig. 4. The change of height above mean sea level against distance over time during the journey from Halfway to Malin Bridge (Red dots are tram stops)

B. The traction forces

In operation, the electric motor of the tram transforms energy, such as the mutual transformation of electricity and kinetic energy, and consequently, provides force for acceleration or deceleration of the tram. The traction force is crucial to the energy calculation and is calculated via (1)

$$F_{traction} = F_{ma} - f_{resistance}, \tag{1}$$

where F_{ma} is the joint force impacted on the tram and $f_{resistance}$ is the total resistance force on the tram.

The joint force is calculated via (2)

$$F_{ma} = M_{tram} a, \tag{2}$$

where M_{tram} is the mass of the tram, reported as 46,500 kg and a is the acceleration of the tram.

The resistance force $f_{\mathrm{resistance}}$ of the tram is the sum of the basic resistance and additional resistance. The basic resistance consists of the motion resistance between the parts of the tram, air resistance, and is also caused by the impact and friction between the wheels and rails. It is calculated via (3) [10]

$$f_1 = a + bv + cv^2, \tag{3}$$

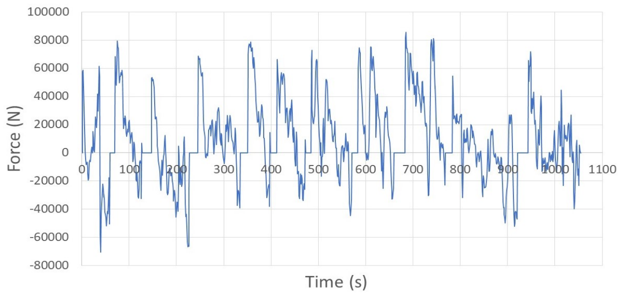

Fig. 5. The traction force and the resistance force of the tram of journey from Halfway to Gleadless Townend

IV. Simulation Model for Energy Balance

MATLAB-Simulink was chosen to construct the model of the tram network. Here, the section of Fitzalan Square to Gleadless Townend is chosen to demonstrate the model structure. As stated in Section II, this tram section will have two trams travelling in the same direction between two adjacent substations at a time. The model consists of substation module 1,2,3, line resistance model R11 to R23, current calculation module and tramcar module, as shown in Fig.6. Once the data is input, the model calculates the current and voltage of different modules, and subsequently the energy used.

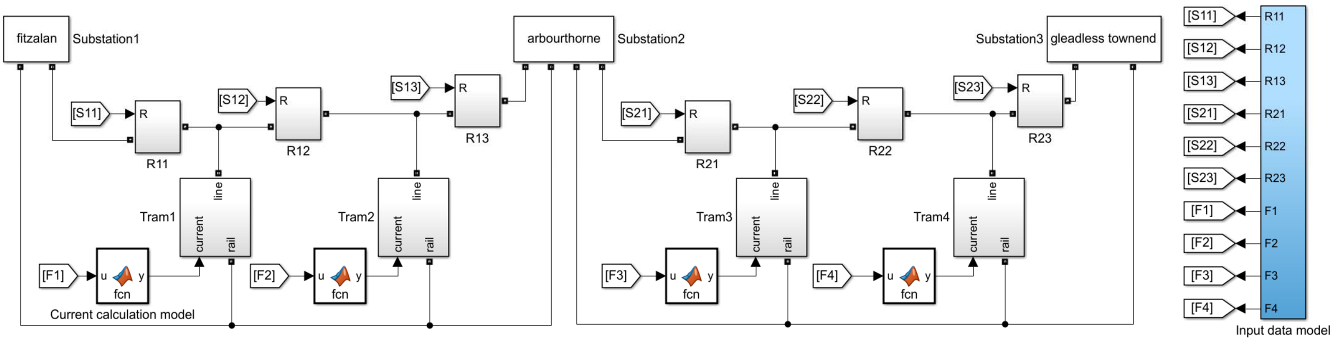

Fig. 6. The tram network model

where v is the velocity, and a, b, c are vehicle-related empirical constant. In this study, a is taken as 2.965, b is taken as 0.23, and c is taken as 0.005. Figures obtained from previous literature on similar systems [10]

Additional resistance is caused by the road condition and consists of ramp resistance, bend resistance and tunnel resistance. The additional resistance is calculated via (4) [11]

$$f_2 = M_{tram} g \sin\left[\tan^{-1}\left(\frac{T_{grad}}{100}\right)\right], \tag{4}$$

where g is the gravity and T_{grad} is the track gradient in percentage and may be obtained from the height above mean sea level

Therefore, the traction force of the tram at any moment during its journey can be known. Using the journey from Halfway to Gleadless Townend as an example, Fig. 5 shows the traction force and the resistance force of the tram during the journey.

A. Substation model

The main component of the substation model is a 24-pulse transformer which is composed of two 12-pulse transformers in parallel. In the ideal condition, the external characteristics of the substation is shown as below in Fig.7 (a). In the figure, U_N stands for Rated voltage, I_N stands for Rated current, and U_E stands for no-load DC output voltage.

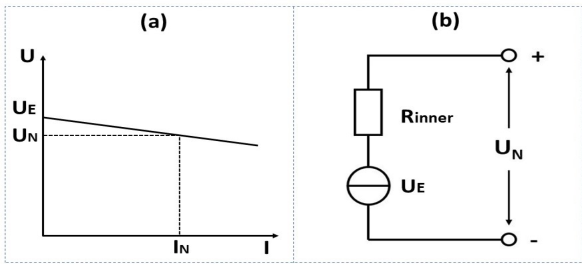

Fig. 7. The external characteristics (a) and the simplified schematic model (b) of the substation

According to the Thevenin equivalent principle, the traction substation can be seen as an equivalent DC voltage source and an internal resistance. Based on this simplified schematic, the substation model shown in Fig.7 (b), the actual substation model is constructed in Simulink, as shown in Fig.8. The U_E is taken as 830V and the (R_{inner}) is taken as 0.02Ω.

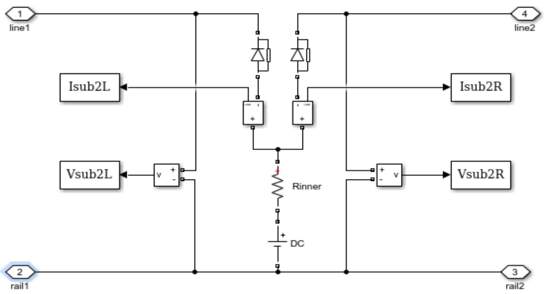

Fig. 8. The actual substation model

B. Line module

The line resistance system is a variable resistor. Its key feature is to work out the catenary resistance according to the travelling distance. However, as there is no variable resistor unit in the library of the 'Specialized Technology', a variable resistor is built. The model is shown in Fig. 9. The resistivity is taken as 8×10^{-5} Ω/m.

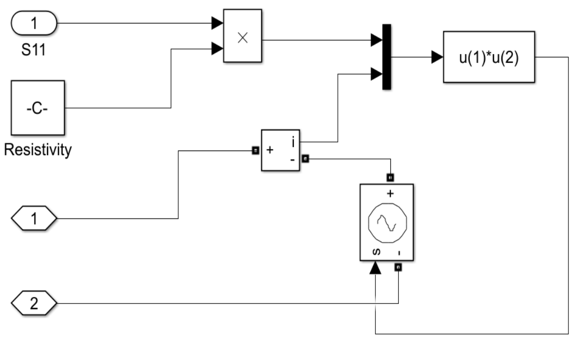

Fig. 9. The line resistance model

C. Current calculation module

The traction motors used in Supertram are the Siemens 1KB2121 and 1KB2021 [12]. Both motors are Asynchronous AC motor / drive combinations, which feature a linear relationship between the rated torque and the rated current (I_e) [13]. Therefore, a linear relationship with the I_e and the force impacted on the motor (F_T) is deduced and can be expressed as (5).

$$I_e = k * F_T, \tag{5}$$

where k is a constant.

According to the reported literature, k can be taken as 18 under traction conditions [14] and 10 under braking for similar tram systems, accounting for drivetrain powerflow efficiencies [15]. Equation (5) was programmed into the model via the Matlab 'Function' module.

D. Tramcar module

As the tram driver controls the motor torque, which is proportional to current, the tram system is replaced and represented by a controllable current source in the model. The on-broad energy 'dump' resistor is also modelled to prevent the catenary voltage raising above the line voltage limit at the tram, while the tram is braking. Commonly, the module employs a constant voltage absorption method using a multiphase IGBT (Insulated Gate Bipolar Transistor) chopper and an absorbing resistor. According to the change of the DC bus voltage during braking, the conduction ratio of the chopper is adjusted, the energy being consumed in the dump resistor is therefore controlled, and the voltage is kept within the limit value. The tram car model is shown in Fig. 10.

The model is constructed according to the working mechanism of the energy dissipation resistor. The resistance of the energy dissipation resistor is set as 0.1 Ω. As the upper limit of the catenary voltage is 900 V, the threshold value of the selector is set as 900. Therefore, when the catenary voltage exceeds 900 V, the IGBT is turned on, leading to energy being dissipated in the dump resistor.

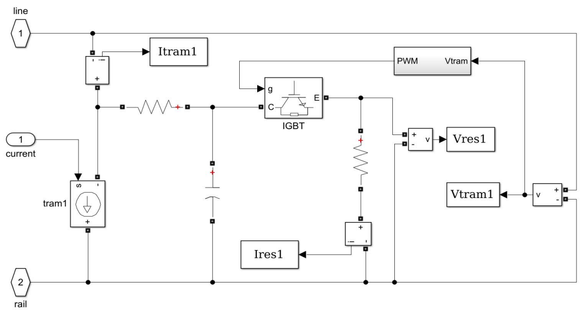

Fig. 10. The tramcar model

V. CALCULATION AND ANALYSIS OF THE ENERGY BALANCE

A. Calculation of the energy balance of a day

Based on the model described above, the voltage and current at the substations and tram together with the energy dissipation in the dump resistor are simulated. From (6), the energy supplied from the substation (E_{sub}), energy consumed in the resistor (E_{res}), and regenerative energy (E_{reg}) of a single journey of a tramcar from Fitzalan Square to Gleadless Townend was calculated.

$$E = \int IV\,dt, \tag{6}$$

where I is the current, V is the voltage, and dt is the time duration.

According to the Supertram timetable, the tram journeys which pass through the Gleadless Townend tram stop are used to illustrate the departure interval and number of departures in a day. Fig. 11 shows the timetable from 06:00 to 00:00 (+1 day) at stop 'Gleadless Townend'. In Fig. 11, the times highlighted with purple are the Purple line trams, and the ones highlighted with blue are of the Blue line trams passing through this stop in one direction.

6-8	8-10	10-12	12-14	14-16	16-18	18-20	20-22	22-24
06:07	08:07	10:10	12:10	14:10	16:10	18:03	20:02	22:02
06:17	08:15	10:15	12:15	14:15	16:15	18:12	20:06	22:17
06:27	08:17	10:22	12:22	14:22	16:22	18:13	20:08	22:22
06:45	08:27	10:34	12:34	14:34	16:33	18:23	20:18	22:37
06:47	08:37	10:45	12:45	14:45	16:43	18:33	20:22	22:42
07:07	08:45	10:46	12:46	14:46	16:45	18:42	20:26	22:57
07:15	08:47	10:58	12:58	14:58	16:53	18:43	20:37	23:02
07:17	08:57	11:10	13:10	15:10	17:03	18:53	20:42	23:17
07:27	09:07	11:15	13:15	15:15	17:12	19:03	20:57	23:22
07:37	09:15	11:22	13:22	15:22	17:13	19:12	21:02	23:37
07:45	09:17	11:34	13:34	15:34	17:23	19:13	21:17	23:52
07:47	09:26	11:45	13:45	15:45	17:33	19:23	21:22	23:56
07:57	09:35	11:46	13:46	15:48	17:42	19:23	21:37	
	09:45	11:58	13:58	15:58	17:43	19:33	21:42	
	09:47				17:53	19:40	21:57	
	09:58					19:44		
						19:58		

Fig. 11. The timetable from 06:00 to 00:00 (+1 day) of stop Gleadless Townend

According to the Fig. 11, the number of departures and the departure interval of the tram journeys between 'Gleadless Townend' and 'Fitzalan Square' are calculated and presented in Fig. 12.

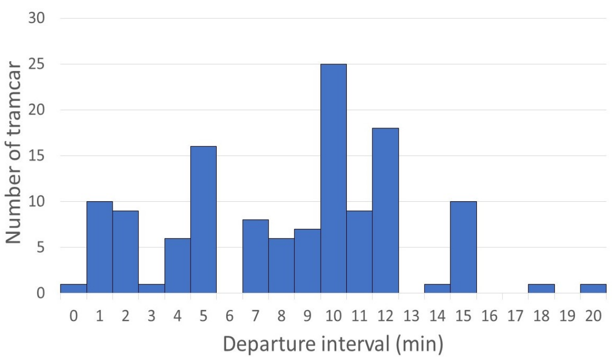

Fig. 12. The number of departures and the departure interval of the tram journey between Gleadless Townend and Fitzalan Square

If the model is run for each set of 'departure intervals', this allows the model to adjust for how much energy is absorbed by a second tram in a track section, if one is present at all. The energies calculated for E_s, E_{res}, and E_{reg} for each 'departure interval' can then be multiplied by the number of departures with this interval, before summing the days energy balance from all the individual 'departure interval' results.

B. *The energy balance of the tram network*

The daily averages of: Energy supply from the substation; Energy lost in Resistive braking, and Energy used by another tram on the track section are calculated to be 41,920kWh, 16,359kWh, and 2,578kWh, respectively. As shown in Fig. 13, the energies calculated based on six sets of data collected are similar. In the entire system, the mean percentage of the regenerative energy utilized by another tram in the section, and that lost in resistive braking is 13.6±1.2% and 86.4±1.2%, respectively. The majority of the braking energy is therefore dissipated in the resistors rather than utilized by other trams. The braking energy also equals to 45.1±0.7% of the energy supplied from the traction substations, clearly making the case for the addition of energy storage to the network.

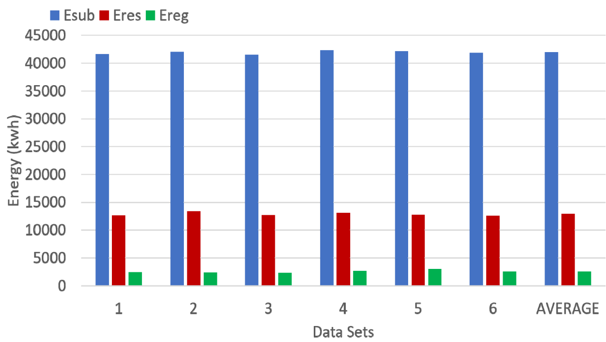

Fig. 13. The energy balance of the tram network calculated based of different data sets

VI. Addition of EV Battery to the Tram Network

The losses associated with the resistive braking could be mitigated with the use of an energy storage system added to the system to absorb some of the regenerated energy generated on tram braking, and supply this back to the track when tram accelerates. Furthermore, given the increasing use of EV's, and the convenient placement of park and ride facilities trackside, synergies between the tram network and the EV batteries used as an Energy storage system (ESS) can now be explored.

A. *Introduction of the ESS*

To demonstrate the effect of adding a simple ESS to the network, an ESS can be added to the Halfway park-and-ride facility in the model. A schematic of the possible configuration is shown is Fig. 14. The addition of the ESS will impact the track section powered by the 'Halfway' substation and the 'Crystal Peaks' substation. The distance between these two substations is 2,300m. A tram car takes approximately 350s to travel along this track section.

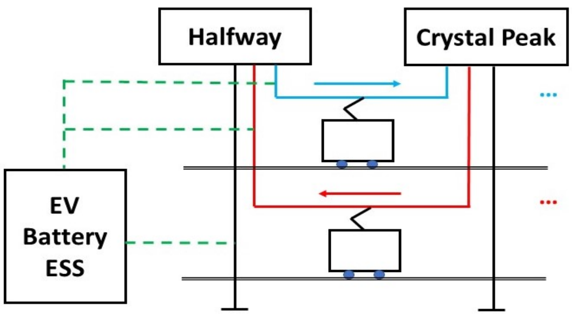

Fig. 14. The schematic of the original model added with ESS

The long-term aim of this project is to show how EV batteries can be used to serve as the ESS in this application. Given that there is much work being carried out on vehicle to grid (V2G) applications (dc-ac conversion). Interestingly, this application could be considered as dc-dc conversion for the proposed R2R scenario, therefore this should be more efficient than standard V2G. In addition, given light rail transport systems are already in existence, their infrastructure could be employed to provide charging stations without additional grid infrastructure if controlled correctly. Since Li-ion batteries are commonly used in EVs, a Li-ion battery is added to the model, to show the effect of EV storage on the tram network energy use.

B. Energy storage system model

The EV battery energy storage module consists of a filter, a bidirectional DC/DC converter, an energy storage inductor and a battery, Fig 15. This module is added to the original model and is connected at the Halfway substation.

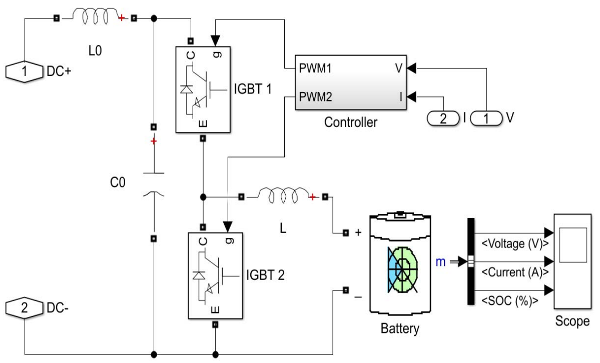

Fig. 15. The model of the energy storage system module in Simulink

The charging and discharging voltage of the ESS are set as 840V and 810V respectively, given that the open circuit voltage of the line is 820V, although this can be adjusted in later work to optimize energy saving against battery size. Operation of the ESS is therefore dependent on the state of the tramcar:

- When the tramcar brakes, the regenerative braking energy is fed back to the catenary and raises the network voltage. The ESS module will then work in "buck" mode. The energy therefore flows from the catenary to the battery;
- When the tramcar is idle, no energy flow between the catenary and the ESS. The ESS module is in standby mode.
- When the tramcar accelerates, the traction network has to supply energy to the tramcar. The catenary voltage is then lowered. The ESS will then work in "boost" mode. The battery then supplies energy to the catenary to lower the energy supplied from a substation.

The impact of the addition of an ESS on the energy balance for the track section powered by the 'Halfway' substation and the 'Crystal Peaks' substation are investigated in this study. Moreover, ESS with various battery capacities (320 V nominal rated voltage and 1C discharge rate limit) are added to the model for understanding the impact of battery capacity on the energy balance. This can help determine the optimal number of parked EVs that could be used for energy storage on the tram network in the future. The ESS capacity is taken as 100Ah, 500Ah, or 1,000Ah, respectively in the initial study.

C. Improvement on energy balance with addition of ESS

The journey of one tramcar, travelling from Halfway (substation 1) to Crystal Peaks (substation 2) is then simulated. The energy balance with and without the addition of ESS can then be calculated.

Fig. 16 shows the catenary voltage during the journey with no addition of ESS. It can be seen that at the start of the simulation the tram voltage and the voltage at substation 1 are equal, whereas by the end of the simulation the tram voltage becomes equal to the voltage at substation 2, as would be expected. Since there is only one tramcar on this section at any one time, when the tram car brakes, the network voltage is raised to above 900 V and hence triggers the resistive dump. In this case, all the braking energy is dissipated by the dump resistor.

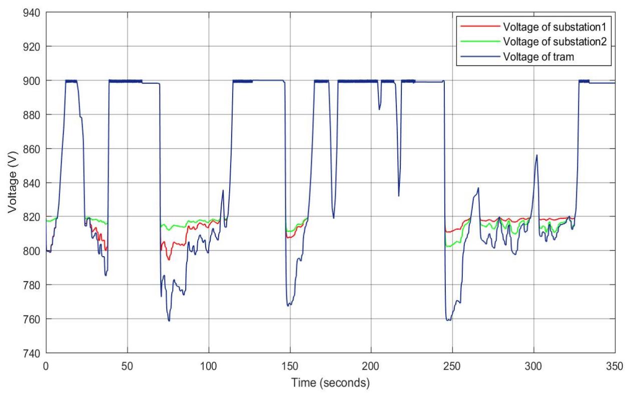

Fig. 16. The tram voltage and voltages at substations during tram journey from Halfway to Crystal Peaks, with no addition of ESS

Fig. 17 shows the energy profile during the journey with no addition of ESS. The total energy supplied from the substations is 15.92kWh per journey and the energy dissipated by the dump resistor is 6.43kWh per journey.

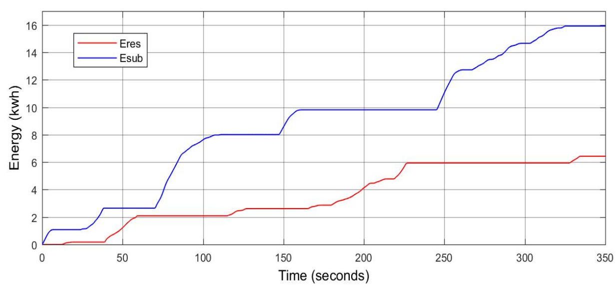

Fig. 17. The energy profile of tram journey from Halfway to Crystal Peaks, with no addition of ESS

An ESS with a 1,000Ah battery is added to the system to demonstrate the impact of addition of ESS on the voltages and the energy profile of the tram journey. Fig. 18 shows the network voltage during the journey with addition of ESS. Similar to that shown in Fig. 16, tram voltage equals the voltage at substation 1 at the start of the simulation and equals the voltage at substation 2 by the end of the simulation. However, with the addition of ESS, part of voltages of the tram and at the substations are substantially smaller than 900V when the tram is braking. This demonstrates that the resistive dump is not triggered since the braking energy flows to the ESS instead of being dissipated in the resistor. Furthermore, when the tram is accelerating, part of voltages with addition of ESS are higher than with no ESS, since the ESS supplies part of the energy required for acceleration. The addition of ESS therefore helps stabilize the voltage.

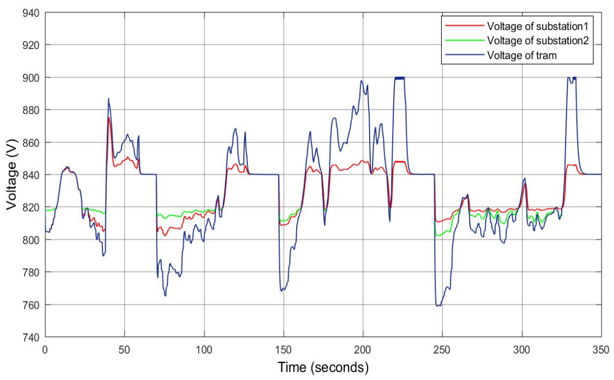

Fig. 18 The tram voltage and voltages at substations during tram journey from Halfway to Crystal Peaks, with addition of ESS

Fig.19 presents the battery (of the ESS) voltage, current and SOC during the tram journey. The discharge rate limit is set as 1C (1000 A). The SOC rise from the original value of 50.00% to 51.13% by the end of the simulation (1 journey).

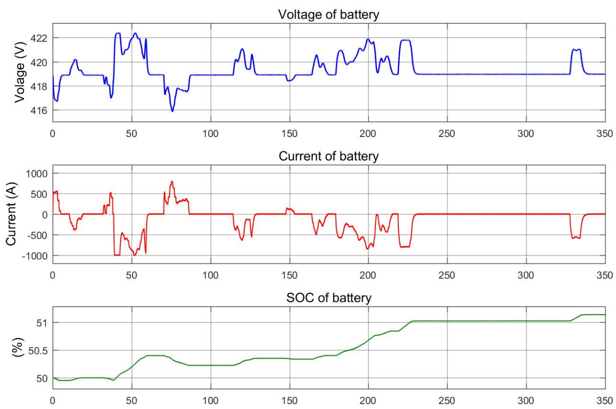

Fig. 19 the battery (of the ESS) voltage, current and SOC during the tram journey

Fig. 20 shows the energy profile of during the journey with addition of ESS. The energy supplied from the substation becomes 14.73 kWh per journey. The energy dissipated by the resistive braking falls to 0.39 kWh per journey.

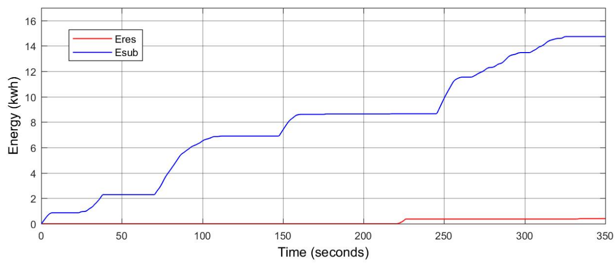

Fig. 20 The energy profile of tram journey from Halfway to Crystal Peaks, with addition of ESS

ESS with different battery capacities are added to the system. The energy balances are shown in Table 1. This illustrates that the bigger the battery capacity, less energy is drawn from the substations and less braking energy is dissipated in the resistor. Comparing to the case with no addition of ESS, the energy supplied from the substation can be reduced by 0.46-1.19 kWh per journey while the energy dissipated in resistive braking can be reduced by 1.84-6.04 kWh per journey. The addition of the ESS recovers 28.6-93.9% of the braking energy. However, these preliminary results reflect the fact that the battery charge / discharge rate is limited to 1C. Allowing a smaller battery capacity to operate at a higher rate may lead to a lower battery capacity requirement, albeit at a reduced lifetime of the battery. The 1C rate was chosen for the preliminary study as this reflects a standard test rate for a battery, and a reasonable rate to charge / discharge a vehicle battery without unduly compromising the vehicle battery lifetime.

Table 1 The energy balance of tram journey from Halfway to Crystal Peaks, with and without addition of ESS (kWh per journey)

	without ESS	with 100Ah	with 500Ah	with 1000Ah
E_{sub}	15.92	15.46	14.82	14.73
E_{res}	6.43	4.59	1.46	0.39

VII. Conclusion

This paper successfully constructed a simulation model of the tram network in Sheffield (UK) in Matlab-Simulink. Purely from GPS data recorded on the tramcars, the energy balance of the entire tram network was investigated. It suggests the braking energy equals to 45.1% of the energy supplied from the substations. The result is close to ~40% which is reported in existing literature for other tram systems [16-19]. Currently, only 13.6% of the braking energy is recovered into other tram operation, the rest 86.4% is dissipated in resistors. With the addition of ESS with a 1,000 Ah battery, 93.9% of the braking energy can be recovered in a tram journey section that has only one tramcar travelling at a time.

The long-term aim of this project is to study the use of EV batteries, through (R2R), to serve as the ESS for the tram network. The work is ongoing and aims to examine the effects of different battery capacities, and optimum placement of park and ride facilities within the tram network. Future studies will also focus on the impact of this application on the lifespan of the EV batteries, and on the economic feasibility and social acceptance of this application.

REFERENCES

[1] UK Paliament, Climate Change Act 2008. 2008: London, UK.

[2] Department for Business, Energy & Industrial Strategy. 2017 UK Provisional Greenhouse Gas Emissions. 2018 Mar 2018]; Available from: https://assets.publishing.service.gov.uk/government/uploads/system/uploads/attachment_data/file/695930/2017_Provisional_Emissions_statistics_2.pdf.

[3] European Commission, Electrification of the Tansport System. 2017, European Commission: Brussell, Belgium.

[4] UTIP, ENERGY EFFICIENCY CONTRIBUTION OF URBAN RAIL SYSTEMS. 2014, Union Internationale des Transports Publics: Brussels, Belgium

[5] Gavin, C., Seasonal variations in electricity demand 2014, Department of Energy & Climate Change London, UK.

[6] Department for Transport, Vehicle Licensing Statistics: Annual 2017 (Revised). 2018, Department for Transport: London, UK.

[7] Zap-Map. CHARGING POINT STATISTICS 2018. 2018 [cited 2018 2018-08-12]; Available from: https://www.zap-map.com/statistics/#charger-type.

[8] Mullan, J., et al., The technical, economic and commercial viability of the vehicle-to-grid concept. Energy Policy, 2012. 48: p. 394-406.

[9] Eltis. Edinburgh's successful Park-and-ride initiative (UK). 2015; Available from: http://www.eltis.org/discover/case-studies/edinburghs-successful-park-and-ride-initiative-uk.

[10] Rochard, B.P. and F. Schmid, A review of methods to measure and calculate train resistances. Proceedings of the Institution of Mechanical Engineers, Part F: Journal of Rail and Rapid Transit, 2000. 214(4): p. 185-199.

[11] Rupp, A., et al., Analysis of a flywheel energy storage system for light rail transit. Energy, 2016. 107: p. 625-638.

[12] Stagecoach. Vehicle Information. 2017 [cited 2018 01-11-2017]; Available from: https://www.stagecoachbus.com/supertram/vehicle-information.

[13] Ruigang, S., et al., Simulation of braking energy recovery for the metro vehicles based on the traction experiment system. Simulation, 2017. 93(12): p. 1099-1112.

[14] Du, F., et al. Modeling and Simulation of Metro DC Traction System with Different Motor Driven Trains. in Power and Energy Engineering Conference (APPEEC), 2010 Asia-Pacific. 2010. IEEE.

[15] Yu, L., et al. Simulation of regenerative braking in DC railway system based on MATLAB/Simulink. in Universities Power Engineering Conference (UPEC), 2010 45th International. 2010. IEEE.

[16] Adinolfi, A., et al., Experimental assessment of energy saving due to trains regenerative braking in an electrified subway line. IEEE Transactions on Power Delivery, 1998. 13(4): p. 1536-1542.

[17] Steiner, M., M. Klohr, and S. Pagiela. Energy storage system with ultracaps on board of railway vehicles. in Power Electronics and Applications, 2007 European Conference on. 2007. IEEE.

[18] Barrero, R., J. Van Mierlo, and X. Tackoen, Enhanced energy storage systems for improved on-board light rail vehicle efficiency. IEEE Vehicular Technology Magazine, 2008. 3: p. 26-36.

[19] Açikbaş, S.l. and M.T. Söylemez. Parameters affecting braking energy recuperation rate in DC rail transit. in ASME/IEEE 2007 Joint Rail Conference and Internal Combustion Engine Division Spring Technical Conference. 2007. American Society of Mechanical Engineers.